Short Communication

Improved Electrochemical Performance of LiMn$_2$O$_4$ /Graphene Composite as Cathode Material for Lithium Ion Battery

Huayun Xu[*]*, Bin Cheng, Yunpo Wang, Long Zheng, Xinhui Duan, Lihui Wang, Jian Yang, Yitai Qian*

Key Laboratory of the Colloid and Interface Chemistry (Shandong University), Ministry of Education, and School of Chemistry and Chemical Engineering, Shandong University, Jinan 250100, PR China
[*]E-mail: xuhuayun@sdu.edu.cn

The electrochemical performance especially rate capability of LiMn$_2$O$_4$ is improved by graphene modified via ultrasonic agitation. The pristine LiMn$_2$O$_4$ and LiMn$_2$O$_4$/graphene composite are characterized by X-ray diffraction (XRD) and transmission electron microscopy (TEM). The obtained LiMn$_2$O$_4$/graphene composite shows reversible capacity of 107 mAh g^{-1} at 50 C charge/discharge rate. At 55 °C, the capacity at 5 C charge/discharge rate for LiMn$_2$O$_4$/graphene is higher than that of pristine LiMn$_2$O$_4$. The electrochemical impedance spectroscopy (EIS) indicates that the charge transfer resistance for LiMn$_2$O$_4$/graphene composite is reduced compared to LiMn$_2$O$_4$ sample.

1. INTRODUCTION

Lithium ion batteries with high rate performance have been considered as potential power sources for electric vehicles and high-power devices [1] . LiMn$_2$O$_4$ spinel as one of the most promising cathode materials attracts extensive attention, due to its low cost, environmental friendliness and good safety [2]. However, the low electronic and ionic conductivities of the electrode materials limit their practical applications [3]. Over past years, extensive effort has been made to enhance the mixed conductivity of electrode materials by admixing high conductive carbon-based materials as conducting networks [4, 5]. Recently, Graphene, a monolayer of carbon atoms, shows superior electrical conductivity, high surface area and good mechanical flexibility [6]. The characteristics provide a highly conductive matrix and offer a high contact area between electrolyte and electrode, facilitating transportation of Li and electrons into the electrode. Thus, incorporating the nanoparticles with the graphene matrix can be an ideal strategy to improve specific capacity and cycling stability [7, 8]. Bak

SM reported nanoscale $LiMn_2O_4$ (10-40 nm) with 27 wt% reduced graphene oxide hybrid as cathode material shows good rate capability [9]. However, so high reduced graphene oxide content means a low volumetric capacity at high charge/discharge rate for their LMO/RGO sample.

In our study, $LiMn_2O_4$ (100 nm around) /graphene composite was tested as a cathode material for lithium ion battery, presenting high conductivity and good rate performance. A high energy density of 393 Wh kg^{-1} was obtained when charge/discharged at 50 C rate for 5 wt % graphene modified $LiMn_2O_4$ sample. Even at 55°C, discharge capacity of 97 mAh g^{-1} at 5C charge/discharge rate was maintained after 100 cycles for $LiMn_2O_4$/5 wt% G sample. The electrochemical impedance spectroscopy (EIS) indicated that the electrode impedance was decreased after modified graphene for $LiMn_2O_4$.

2. EXPERIMENTAL

2.1. Synthesis

The $LiMn_2O_4$ was prepared by the sol–gel method using citric acid and glycol as the chelating agent. The stoichiometric amount of $LiNO_3$ and 50 wt% $Mn(NO_3)_2$ solution were mixed with citric acid and glycol which their molar ratio was kept as 1:4 dissolved in 20 mL of distilled water. The molar ratio of metal ion to citric acid was 1:1. Then the solution was stirred at 80 °C for 2 h, and the obtained gel was dried at 180 °C for 10h. After that, it was sintered at 700 °C for 10 h. Graphene nanosheets, which were prepared by a chemical exfoliation process [10], were mixed with $LiMn_2O_4$ in ethanol solution with ultrasonic agitation and then sintered at 300 °C for 3h under argon atmosphere.

2.2. Characterization

XRD patterns of the samples were provided using a Bruker D8 advanced X-ray diffractometer with Cu Kα radiation (λ=1.5418 Å). The $LiMn_2O_4$/graphene composite was observed on a transmission electron microscope (TEM, JEOL-2010). The coin cells comprised of the prepared powder as cathode, lithium as anode, and an electrolyte having 1M $LiPF_6$ in an ethylene carbonate (EC)-diethyl carbonate (DEC)-ethyl methyl carbonate (EMC) mixture (1:1:1). Micro-porous polypropylene separator was used in those cells. The cell preparation was carried out in an Ar-filled dry box. The charge/discharge cycles for assembled cells were measured using a Land CT2001 battery tester. EIS were performed by a Zahner Elektrik IM6 (Germany) impedance instrument over the frequency range of 100 kHz to 0.01Hz.

3. RESULTS AND DISCUSSION

3.1. Structure and morphology

Figure 1 shows the XRD patterns of the $LiMn_2O_4$, $LiMn_2O_4$/2 wt% G, $LiMn_2O_4$/5 wt% G and graphene nanosheets. The diffraction peaks (Figure 1a-1c) can be ascribed to cubic $LiMn_2O_4$ with a

space group of Fd3-m, except the peak at $2\theta = 26.5°$ that can be assigned to the (002) plane of graphene sheets (Figure 1d). And this peak strengthens with the increase of graphene for $LiMn_2O_4$/G composite. Figure 2 shows the TEM image of (a) Graphene, (b) $LiMn_2O_4$, (c) $LiMn_2O_4$/2 wt% G and (d) $LiMn_2O_4$/5 wt% G. It can be seen that the particle size of $LiMn_2O_4$ is around ~ 100 nm (Figure 2b) and uniformly dispersed on the surface of graphene nanosheets as shown in Figure 2c and 2d.
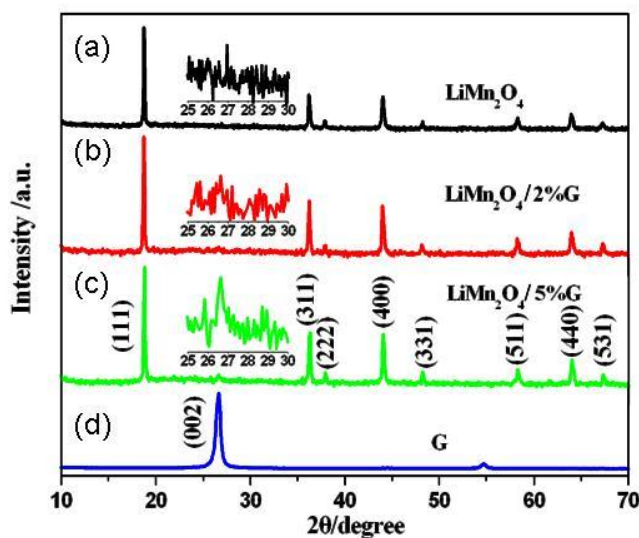
Figure 1. XRD patterns of (a) $LiMn_2O_4$, (b) $LiMn_2O_4$/2 wt% G, (c) $LiMn_2O_4$/5 wt% G and (d) Graphene.
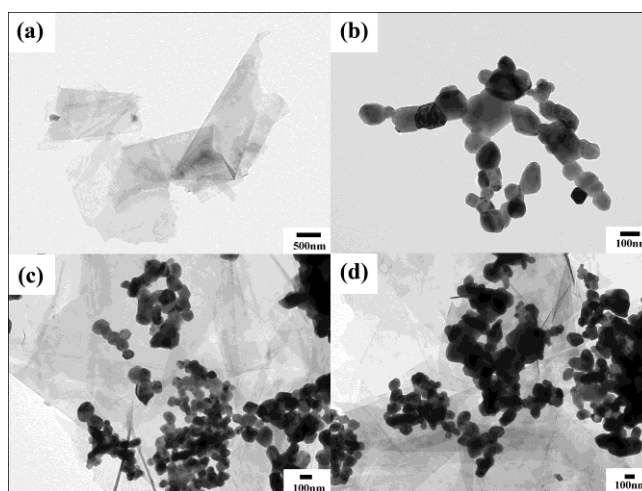
Figure 2. TEM of (a) Graphene, (b) $LiMn_2O_4$, (c) $LiMn_2O_4$/2%G, (d) $LiMn_2O_4$/5%G

3.2. Electrochemical Characterization

The cycle property of the pristine $LiMn_2O_4$ and $LiMn_2O_4$/G samples were performed with varied charge/discharge rate as given in Figure 3a. $LiMn_2O_4$/G samples performs improved rate

capability especially for $LiMn_2O_4/5$ wt % G sample which shows 107 mAh g^{-1} capacity when charged/discharged at 50 C rate, while only 80 mAh g^{-1} is obtained for pristine $LiMn_2O_4$ sample.

A higher rate performance was investigated for $LiMn_2O_4/5$ wt% G sample as given in Figure 3b. Even at 80 C charge/discharge rate, almost 60 mAh g^{-1} capacity is obtained. The charge/discharge curves for $LiMn_2O_4/5$ wt% G sample at different rate were shown in Fig. 3c. Seen from Figure 3d, the electrochemical performance of $LiMn_2O_4/G$ is also improved compared to pristine $LiMn_2O_4$ sample at 55 °C. At 5C charge/discharge rate, about 97 mAh g^{-1} capacity after 100 cycles is maintained for $LiMn_2O_4/5$ wt% G, which is higher than that of pristine $LiMn_2O_4$. Yue synthesized $LiMn_2O_4/C$ composite and obtained discharge capacity of 83 mAh g^{-1} at the current density of 2 A g^{-1}[11]. Jia reported that they achieved $LiMn_2O_4/CNT$, which exhibited reversible capacity of 85 mAh g^{-1} at 1C [12]. Liu also synthesized $LiMn_2O_4/CNT$ by sol-gel route and discharge capacity of 31 mAh g^{-1} was achieved at the rate of 13 C[13]. Bak synthesized $LiMn_2O_4/RGO$ nanocomposite and reversible capacity of 101 mAh g^{-1} at 100 C was obtained[14]. They found there was a large surface charge storage contribution for this good rate capability. Although the electrochemical property for $LiMn_2O_4/5$ wt% G sample in our work doesn't exceed Bak' result but it is comparable to Patey's result[15], and, is superior to Yue, Jia and Liu's reported results.
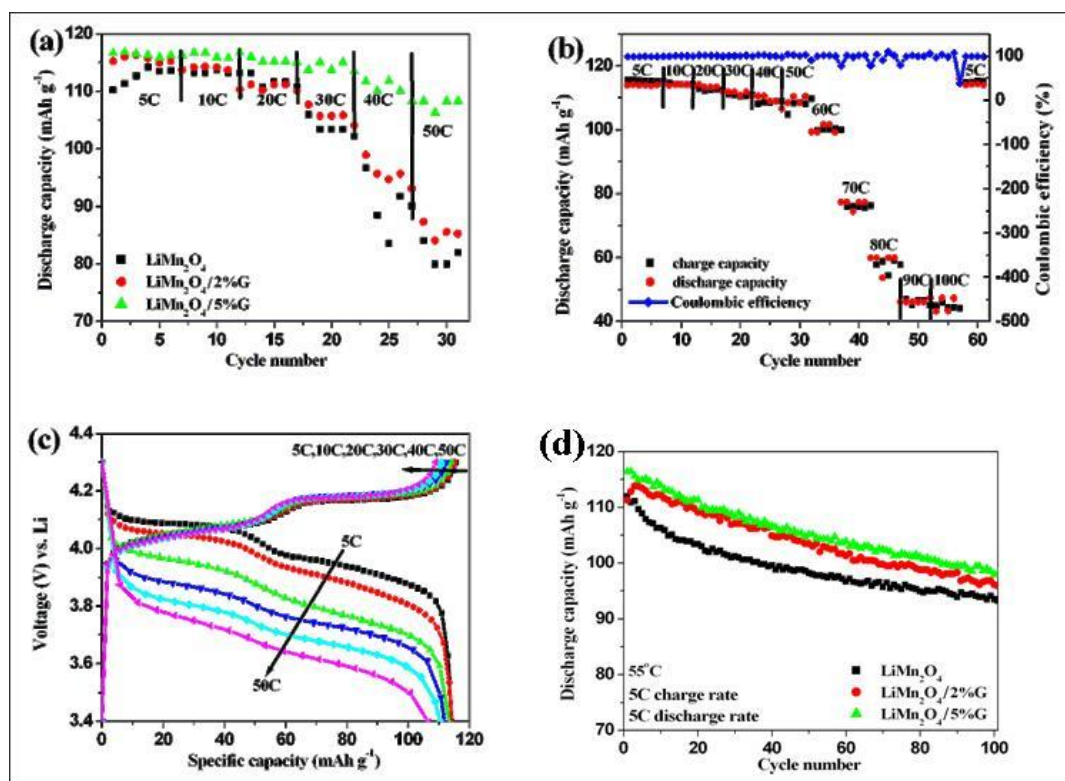

Figure 3. (a) Compared rate capability of $LiMn_2O_4$ and $LiMn_2O_4/G$ samples as a function of C rate, (b) Rate capability of $LiMn_2O_4/5$ wt% G samples as a function of C rate, (c) Charge-discharge curves for $LiMn_2O_4/5$ wt% G samples at different rate, (d) Discharge capacity as a function of cycle for $LiMn_2O_4$ and $LiMn_2O_4/G$ samples at 55 °C.

EIS was performed to investigate the electrode resistance changes for $Li/LiMn_2O_4$ and $LiMn_2O_4/G$ samples as presented in Figure 4. The intercept at the real (Z') axis in high frequency corresponds to the ohmic resistance (R_e). The semicircle in the middle frequency range indicates the charge transfer resistance (R_{ct}) and the inclined straight line relates to the Warburg impedance (Z_w) [16]. Seen from Fig. 4, the R_{ct} value of the $LiMn_2O_4$, $LiMn_2O_4/2$ wt% G and $LiMn_2O_4/5$ wt% G sample is 165, 126 and 75 Ω, respectively. Clearly, the $LiMn_2O_4/graphene$ sample can suppress the charge transfer resistance, which is contributed to a higher discharge capacity and high rate capability compared to the pristine $LiMn_2O_4$ sample (shown in Figure 3).
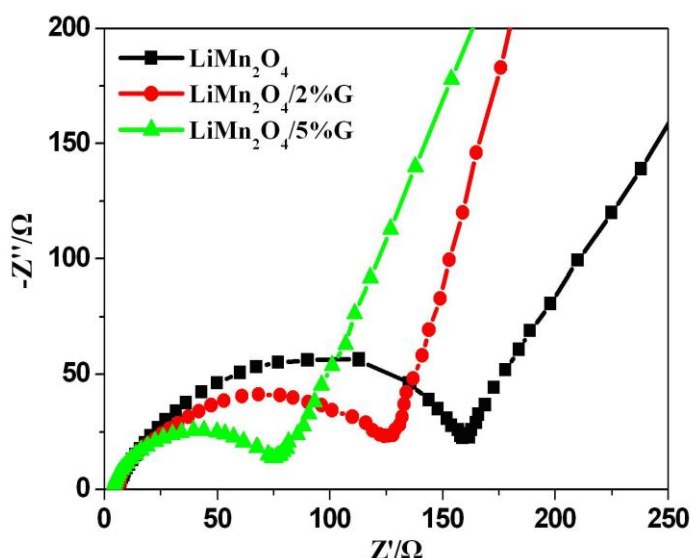

Figure 4. Nyquist plots of $LiMn_2O_4$, $LiMn_2O_4/2$ wt% G and $LiMn_2O_4/5$ wt% G samples

4. CONCLUSIONS

$LiMn_2O_4$ particles were modified by graphene nanosheets using ultrasonic agitation method. The obtained $LiMn_2O_4/graphene$ composite performs a reversible capacity of 107 mAh g^{-1} at 50 C charge /discharge rate, The electrochemical properties of $LiMn_2O_4/graphene$ composite at 55°C are also improved in this work. Greatly enhances of the electrical conductivity due to graphene and efficient use of the $LiMn_2O_4$, leading to an outstanding electrochemical performance of the hybrid cathodes.

References

1. J.B. Goodenough, and Y. Kim, *Chem. Mater.* 22 (2010) 587-603.
2. X.W. Li, R. Yang, B. Cheng, Q. Hao, H.Y. Xu, J. Yang, Y.T. Qian, *Mater Lett*, 66 (2012) 168-171.
3. A. Yamada, H. Koizumi, S.I. Nishimura, N. Sonoyama, R. Kanno, M. Yonemura, T. Nakamura, Y. Kobayashi, *Nat. Mater.* 5 (2006) 357-360.
4. Y.G. Wang, Y.R. Wang, E.J. Hosono, K.X. Wang, H.S. Zhou, Angew. *Chem. Int. Ed.* 47 (2008) 7461-7465.
5. Y. Zhou, J. Wang, Y. Hu, R.O. Hayreb, Z. Shao, *Chem. Commun.* 46 (2010) 7151-7153.
6. Y. Sharma, N.G. Sharma. V. Subba, B. Rao, V.R. Chowdari, *Electrochim. Acta,* 53 (2008) 2380-2385.
7. Y. Wang, Z.S. Feng, J.J. Chen, *Mater Lett*, 71 (2012) 54-56.
8. X. Zhao, C.M. Hayner, H.H. Kung, *J. Mater. Chem.* 21 (2011) 17297- 17303.
9. S.M. Bak, K.W. Nam, C.W. Lee, K.H. Kim, H.C. Jung, X.Q. Yang, K.B. Kim, *J. Mater. Chem.* 21 (2011) 17309-17315.
10. X.F. Zhou, Z.P. Liu, *Chem. Commun.* 46 (2010) 2611-2613.
11. H. J. Yue, X. K. Huang, Do. P. Lv, Y. Yang. *Electrochim. Acta*, 54 (2009) 5363-5367.
12. X. L. Jia, C. Z. Yan, Z. Chen, Y. F. Lu. *Chem. Commun.*, 47 (2011) 9669-9671.
13. X. M. Liu, Z. D. Huang, S. Oha. *J. Power Sources*, 195 (2010) 4290-4296.
14. S. M. Bak, K. W. Nam, C. W. Lee, K. B. Kim. *J. Mater. Chem.*, 21 (2011) 17309- 17315.
15. T. J. Patey，R. Büchel, S. H. Nga, F. Krumeich, S. E. Pratsinis，P.Novák. *J. Power Sources*, 189 (2009) 149-154.
16. M.D. Levi, D. Aurbach, *J. Phys. Chem. B*, 101 (1997) 4630-4640.